Electrical Investigation of Wake-Up in High Endurance Fatigue-Free La and Y Doped HZO Metal–Ferroelectric–Metal Capacitors

Amey M. Walke, Mihaela I. Popovici, Kaustuv Banerjee, Sergiu Clima, Pankaj Kumbhare, *Member, IEEE*, Johan Desmet, Johan Meersschaut, Geert Van den Bosch, Romain Delhougne, Gouri Sankar Kar, and Jan Van Houdt, *Fellow, IEEE*

***Abstract*— High endurance of 10^{11} cycles is demonstrated in ~9–10-nm stoichiometric Hafnium Zirconate (HZO) metal–ferroelectric–metal (MFM) capacitors deposited using Cl precursors with La and Y dopants. La doping is shown to offer higher remnant polarization than Y. Investigation of doped layers with asymmetric polarization versus electric field (P–E) measurements and unipolar fatigue cycles suggests that in the pristine state, the HZO is comprised of ferroelectric domains with internal built-in electric field-induced pinned coercive field (E_c). Doping is shown to increase the pinning effect and two distinct groups of ferroelectric domains emerge, which is antialigned at zero applied electric field (E). The antiferroelectric-like (pinched P–E loop) behavior is therefore attributed to internal built-in E-induced pinning of the domains during growth and/or annealing steps. The initial wake-up is attributed to gradual depinning of the domains with bipolar electric pulses. Suppression of monoclinic phase was observed in doped layers that survive 10^{11} cycles. The wake-up is shown to be dependent on total duration and magnitude of bipolar electric pulses. Precycling scheme is demonstrated for stable operation at a lower field.**

***Index Terms*— Antiferroelectric like HZO, HZO metal–ferroelectric–metal (MFM) capacitors, La and Y doped HZO, wake-up.**

I. Introduction

HF- AND Zr-based mixed binary oxides have attracted the attention of several research groups [1]–[5] due to compatibility with CMOS processing and growth techniques such as atomic layer deposition (ALD). Hafnium Zirconate (HZO) is being explored for both ferroelectric field effect transistor (FEFET) [6]–[8] and ferroelectric random access memory (FERAM) [4], [9], [10] applications. Ferroelectricity in HZO has been demonstrated with Si [11], Al [11], as well as La [12]–[14] dopants. In the undoped form, the coercive field of HZO layers is within ~0.9–1.2-MV/cm range, which drops with addition of dopants in the layers to 0.5–0.7 MV/cm [12]. Doping, therefore, allows reduction in the field of operation thereby extending endurance by several orders of magnitudes. The extended endurance also comes at a cost of pinched polarization versus electric field (P–E) loops in the pristine state as well as a prolonged wake-up effect [12]. There are several reports where HZO is most popularly grown with metal-organic precursors [1]–[5], [8], which are inherently susceptible to unintentional C incorporation into the grown films [15], which is known to influence its ferroelectric response. In this work, we explore Y and La doping in the HZO films grown with Cl-based precursors to avoid unintentional carbon doping typically found in films deposited using metal-organic precursors and likely responsible for leakage and earlier breakdown. Furthermore, pinched P–E loop behavior is investigated through asymmetric P–E measurements and wake-up is investigated through unipolar and bipolar fatigue measurements.

Manuscript received 5 April 2022; revised 18 May 2022; accepted 23 June 2022. Date of publication 12 July 2022; date of current version 25 July 2022. This work was supported by the IMEC's industry affiliated program. The review of this article was arranged by Editor B. Iñiguez. *(Corresponding author: Amey M. Walke.)*

Amey M. Walke, Mihaela I. Popovici, Kaustuv Banerjee, Sergiu Clima, Johan Desmet, Johan Meersschaut, Geert Van den Bosch, Romain Delhougne, and Gouri Sankar Kar are with the IMEC, 3001 Leuven, Belgium (e-mail: amey.walke@imec.be).

Pankaj Kumbhare was with IMEC, 3001 Leuven, Belgium. He is now with the Ministry of Electronics and Information Technology, Government of India, New Delhi 110003, India.

Jan Van Houdt is with the IMEC, 3001 Leuven, Belgium, and also with the KU Leuven, 3001 Leuven, Belgium.

Color versions of one or more figures in this article are available at https://doi.org/10.1109/TED.2022.3186869.

Digital Object Identifier 10.1109/TED.2022.3186869

II. Experiment

TiN/HZO/TiN metal–ferroelectric–metal (MFM) capacitors were fabricated on 300-mm p^{++} Si (100) wafers with different concentrations of Y and La dopants. First, the bottom (10 nm) metal (TiN) electrode was deposited using ALD at 450 °C. Next, 95 ± 5 Å HZO was deposited at 300 °C using $HfCl_4$ and $ZrCl_4$ as precursors and H_2O as oxidant. Doping with La and Y uses $La(EtCp)_2(^iPr\text{-}AMD)$ and $Y(^iPrCp)_3$ precursors and H_2O oxidant and the binary La_2O_3 and Y_2O_3 were deposited at 250 °C and 270 °C, respectively, in adjacent reactors. The pulse times are of the order of a few seconds, while the purge times are two times larger, as typically used in ALD processes. All depositions were made *in situ* by alternatively shuffling the 300-mm wafers between the reactors where HZO depositions are performed. The areal density (atoms/cm^2) of La, Y, Hf, and Zr was evaluated by the Rutherford backscattering spectroscopy (RBS). Y concentration was measured

0018-9383 © 2022 IEEE. Personal use is permitted, but republication/redistribution requires IEEE permission.
See https://www.ieee.org/publications/rights/index.html for more information.

Authorized licensed use limited to: IMEC. Downloaded on September 12,2022 at 07:24:23 UTC from IEEE Xplore. Restrictions apply.

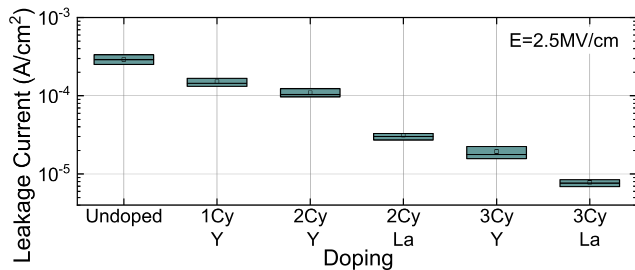

Fig. 1. DC leakage at $E = 2.5$ MV/cm through (~30/wafer) MFM capacitors with different concentrations of Y and La dopants.

in HfO2 films as Zr and Y cannot be separated by RBS measurements. The concentration of dopant was evaluated at ~0.5% (1 cy Y dopant), 1% (2 cy Y dopant), and 1.5% (3 cy Y dopant) and 1.7% (3 cy La dopant) with an error of ~±0.15% for both dopants. The concentration of Cl was found to be 2.7% ± 1.18% on a reference 95 Å La doped HZO sample deposited on a Si substrate to eliminate signal of Cl coming from the bottom TiN electrode. The top metal (TiN) electrode was deposited in two steps. First, 10-nm TiN was deposited with 2-nm Si cap followed by annealing in N_2 ambient at 550 °C. Next, the Si cap was removed and the 20-nm TiN layer was deposited by the same process as before. The deposited layers were further characterized by grazing incidence X-ray diffraction (GIXRD). The top TiN electrode was patterned by reactive ion etching process to form MFM capacitors with an area of 4800 μm^2.

Polarization versus electric field (P–E) loops and fatigue measurements were performed using TFA 3000 system. The bottom electrode was contacted through bottom of the highly p-type doped substrate. P–E loops were measured using a triangular waveform with a frequency of 10 kHz. Bipolar (or unipolar) trapezoidal pulses were applied for fatigue measurements with rise, fall, and flat time of 200 ns each. Both fatigue and P–E measurement pulses were applied to the bottom electrode from back side of the wafer, whereas measurements were performed from the top electrode. The electric field is calculated by dividing the applied bias by thickness of the layer.

III. Results and Discussion

Fig. 1 shows the comparison of dc leakage (at $E = 2.5$ MV/cm, ~35 devices/wafer) through different MFM capacitors as a function of doping concentration. The leakage decreases with increase in number of dopant cycles (Cy). Moreover, La doping offers lower leakage than Y dopant for the same number of doping cycles.

GIXRD spectra [see Fig. 2(a)] show that films are well crystallized with the main diffraction peak around the value of 30.5°, which could indicate the presence of orthorhombic phase as o(111). Moreover, the weak diffraction peak at ~28.5° characteristic to m(−111) monoclinic phase disappears when dopants are embedded in the HZO layer.

A comparison of the endurance behavior for different concentrations of Y and La dopants is shown in Fig. 3. The endurance improves when the number of dopant cycles increases from 0 to 3 cycles, which is also consistent with the leakage in the pristine state (see Fig. 1). As expected, the

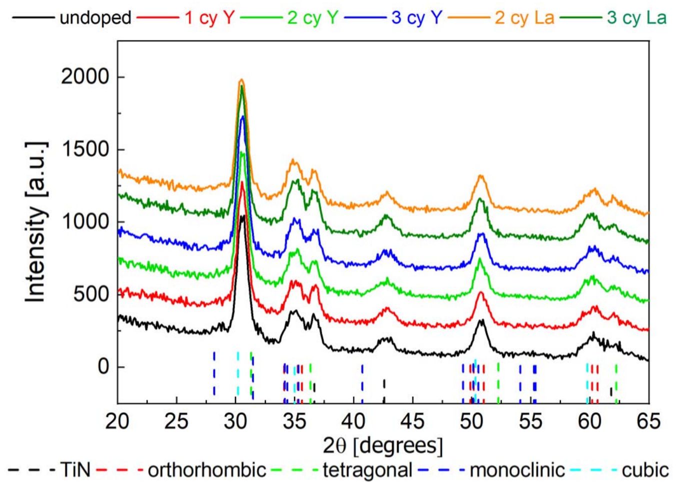

Fig. 2. GIXRD plots for different concentrations of Y and La dopants. The peak corresponding to monoclinic phase decreases as Y and La doping is increased from 0 to 3 cycles.

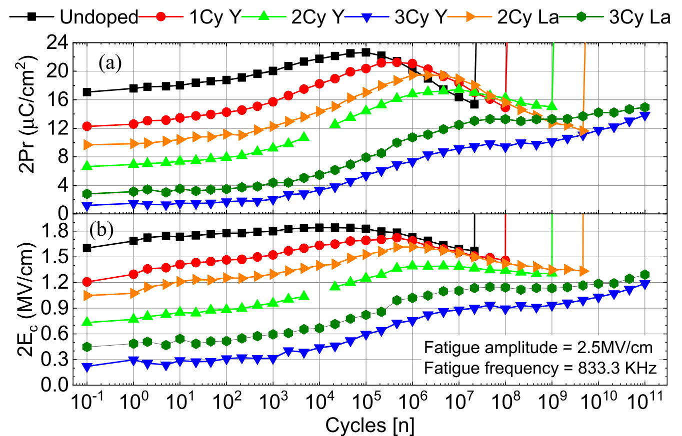

Fig. 3. (a) Evolution of $2P_r$ and (b) $2E_c$ as a function of fatigue cycles with different numbers of Y and La doping cycles. The first entry (0.1 cycles) corresponds to the pristine state response.

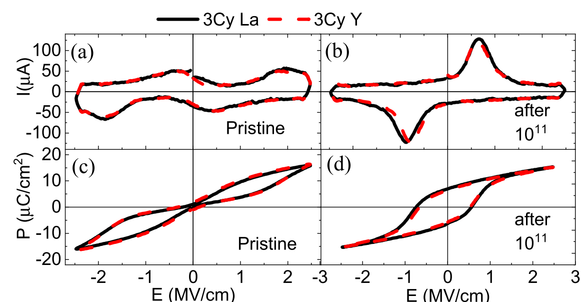

Fig. 4. (a) and (b) I–E loop and (c) and (d) corresponding P–E loops before (a) and (c) and after (b) and (d) 10^{11} cycles.

coercive field (E_c) field decreases with increase in the doping concentration. La doping is shown to offer higher $2P_r$ and $2E_c$ at the same number of doping cycles compared to Y. This can be attributed to larger ionic radius of La^{3+} (1.16 Å) offering higher distortion of the unit cell compared to a smaller (1.02 Å) Y^{3+} ion. Fig. 4 shows the I–E and P–E loops before and after 10^{11} cycles. No impact of leakage on the measurement is observed after 10^{11} cycles. In the pristine state, the current versus electric field (I—E) loop shows multiple peaks, which merges to form a single peak by 10^{11} cycles.

Authorized licensed use limited to: IMEC. Downloaded on September 12,2022 at 07:24:23 UTC from IEEE Xplore. Restrictions apply.

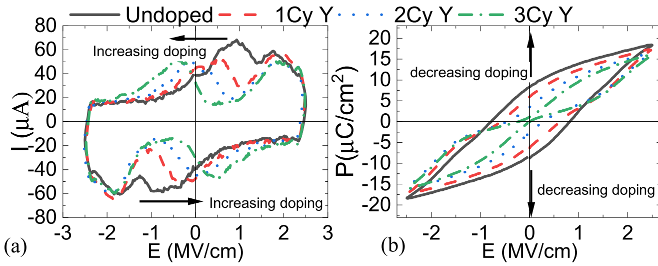

Fig. 5. Pristine state (a) I–E and (b) P–E loops as a function of Y doping cycles. Multiple current peaks appear with increasing separation as doping increases.

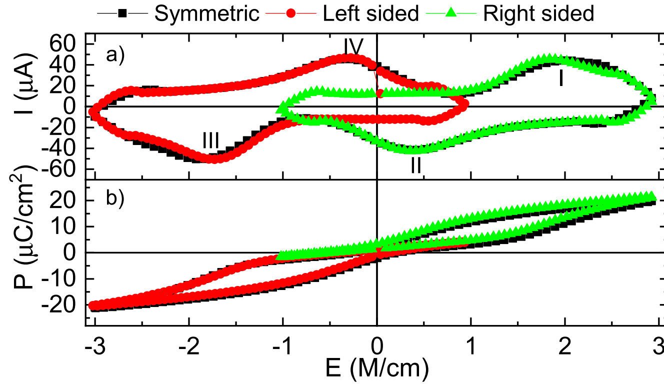

Fig. 6. Symmetric and asymmetric (a) I–E and (b) P–E measurements on 3 Cy La doped HZO MFM capacitors showing two groups of ferroelectric domains with shift in coercive fields.

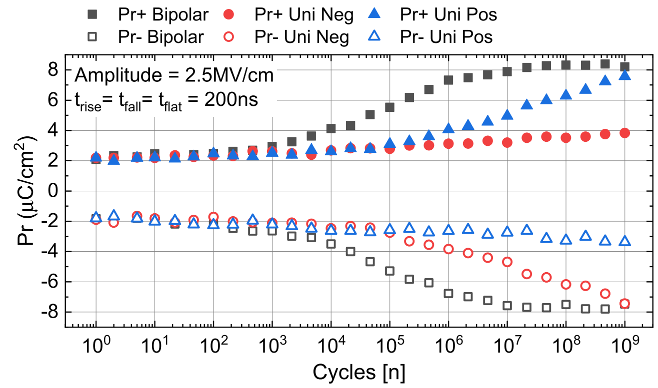

Fig. 7. Evolution of positive and negative remnant polarization with unipolar (positive or negative) and bipolar electric field cycles. Measurements were performed on 3 Cy La doped HZO MFM capacitors.

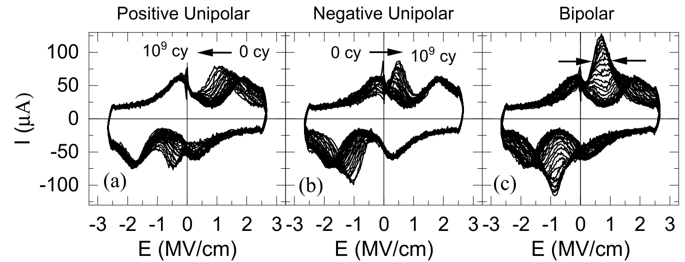

Fig. 8. I–E loop evolution under the application of (a) positive, (b) negative unipolar, and (c) bipolar electric field cycles. The evolution is shown from pristine state (0 cycles) until 10^9 cycles.

The separation between current peaks in pristine state increases with increase in the dopant concentration, as shown in Fig. 5(a). At the same time, the P–E loops are more and more pinched at $E = 0$ as doping concentration is increased. At 3 Cy doping, the P–E loop appears to be like an antiferroelectric material.

Fig. 6 shows symmetric (+3 to −3 MV/cm) and asymmetric (+3 to −1 MV/cm and −3 to +1 MV/cm) I–E and P–E measurements performed on 3 Cy La doped HZO MFM capacitors. Asymmetric measurements show the existence of two groups of ferroelectric domains with shift in the coercive field. In other words, the coercive field of the two groups of domains is asymmetrically pinned. During symmetric P–E measurements, at $E = 0$, both groups have opposite alignment of dipoles resulting in cancellation of net polarization. As a result, pinching is observed in the P–E loops.

In order to establish that the two groups of domains are different and independent of each other, we perform bipolar and unipolar fatigue measurements. Fig. 7 shows the evolution of positive and negative P_r as a function of unipolar and bipolar fatigue cycles. Unipolar fatigue cycling results in an asymmetric wake-up and bipolar electric field cycling is necessary for faster and symmetric wake-up of the doped layers. Fig. 8 shows a closer look at evolution of previously identified two groups of domains under application of symmetric bipolar and asymmetric (unipolar) fatigue cycles. Fatigue cycling seems to gradually remove the built-in electric field making the positive and negative coercive more equal in magnitude. Removal of the built-in field results in merging followed by narrowing of the switching current peaks.

Fig. 9(a) shows the evolution of coercive field extracted from the peak position of the switching currents of three-cycle La doped film capacitors up to 10^{11} cycles. Two groups of domains show distinct switching current peaks until 10^5 cycles. Between 10^5 and 10^9 cycles, switching peaks merge to form a single peak and narrowing is observed. Beyond 10^9 cycles, further narrowing of the current peaks is seen. $2E_c$ values can be extracted by subtraction of up and down coercive field and are plotted in Fig. 9(b). The $2E_c$ value of two groups of domains is similar at the beginning as well as toward the end of the fatigue cycling.

These experiments suggest the following.

1) The doping results in pinning of the coercive field and distribution of the domains in two (or more) independently switching groups.

2) Each pinned group evolves with only one polarity of fatigue cycles and bipolar cycles evolve both groups of domains symmetrically. Each group has only two stable states (i.e., up and down polarization state) and the two groups can be switched independent of each other.

3) Similar $2E_c$ values before and after merging of the switching current peaks [see Fig. 9(b)] suggest that the two groups of domains have a similar phase composition before and after wake-up.

There have been several reports on investigation of pinched loop and wake-up behavior of HZO layers [16]–[23]. Phenomenologically, the pinched loop behavior can be modeled as a triple valley system in the Gibbs free energy versus polarization landscape [17]. At the microscopic level, the following mechanisms have been proposed: the presence of

Authorized licensed use limited to: IMEC. Downloaded on September 12,2022 at 07:24:23 UTC from IEEE Xplore. Restrictions apply.

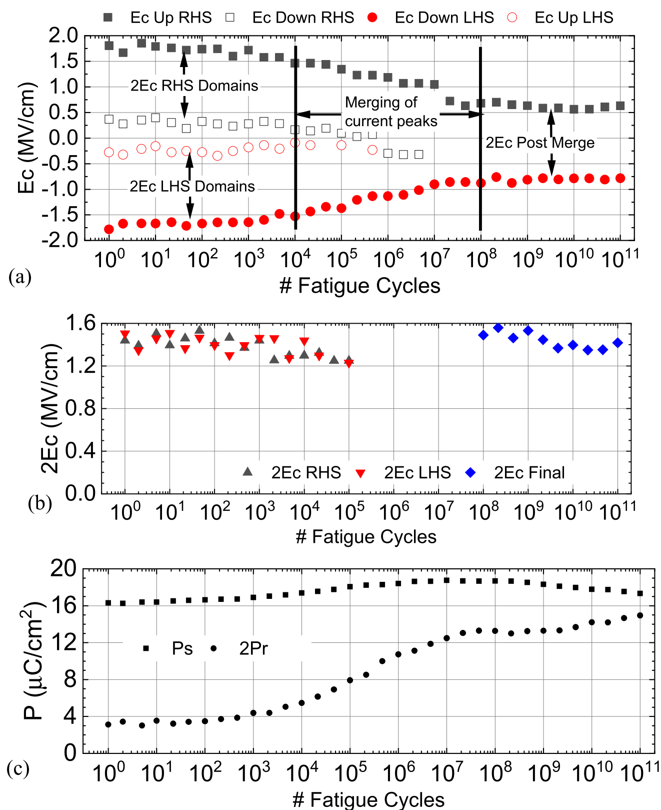

Fig. 9. (a) Evolution of coercive field of three-cycle La doped HZO film as a function of bipolar fatigue cycles. Square points correspond to RHS group of domains and circle points correspond to coercive field of LHS group of domains. (b) Extracted $2E_c$ for LHS and RHS groups of domains as a function of fatigue cycles. The $2E_c$ values are similar for both groups both before and after wake-up (i.e., after merging of current peaks with cycling) suggesting that the two groups are likely to be composed of the same ferroelectric phase with shifted coercive field. (c) P_s and $2P_r$ as a function of fatigue cycles. Change in P_s as a function of cycles is less, compared to $2P_r$.

either antialigned pinned dipoles [22], [24] [25] or electric field-induced reversible phase conversion from nonpolar to polar phase [20], [26]–[28]. The second mechanism is also accompanied by a depolarization field model to explain wake-up behavior [29]–[31].

The electric field-induced reversible phase transition from nonpolar to polar phase has been widely investigated in experimental studies using the synchrotron XRD technique [20], piezo response force microscopy [26], and scanning transmission electron microscopy in annular brightfield mode (STEM-ABF) techniques [32]. Two models for pinched loop using depolarization field were discussed in [29]. The first model assumes the electric field-induced reversible phase transformation process where a hysteron with three states of polarization ($P = 0$, $+P_r$, and $-P_r$) in combination with depolarization field created by paraelectric phases present in series with the ferroelectric phases. The wake-up effect is explained by reduction in the depolarization field due to gradual removal of charged defects or phase conversion of the paraelectric layer [29]–[31]. This model implies that each hysteron with three states contributes to all switching current peaks in the I–E loop. Therefore, it creates I–E loops with the same switching charge in each of the switching current peaks. Any asymmetry due to addition of defect or charge is expected to impact all transitions between three states of the hysteron. Furthermore, a permanent phase transition during fatigue cycling would also impact all four switching current peaks. Therefore, each three-state hysteron is expected to respond to both positive and negative electric field cycles. Our unipolar fatigue measurements show that only one pair of the current peak [either I and II or III and IV in Fig. 6(a)] responds to a given polarity of the fatigue field cycles. This implies that the hysterons that respond to positive electric field and those that respond to negative electric field are not the same. Therefore, a three-state hysteron model needs an additional investigation to understand the unipolar fatigue cycling behavior seen in our devices.

The second model evaluated in [29] assumes a ferroelectric layer (with two stable polarization states $+P_r$ and $-P_r$) in series with a paraelectric layer. The paraelectric layer can be a nonpolar phase, interfacial oxide layers at the electrode interfaces, or finite screening length in metal electrodes. In addition, an internal electric field was assumed that shifts the coercive field, thereby delaying nucleation of switching. The wake-up is attributed to either changes in the thickness of paraelectric layer or charge trapping and detrapping processes. Our experiments are consistent with this second model where the ferroelectric domains with two stable states are split into two groups. One group is subjected to positive internal field and another one is subjected to negative internal field. This model is also consistent with unipolar fatigue measurements, which only affects one group of domains independent of the other. Moreover, it also explains the same value of $2E_c$ extracted before and after wake-up.

Other mechanisms include an irreversible phase conversion from nonferroelectric to ferroelectric phases [33], [34] or 90° reorientation of dipoles [28], [35]. In [33], global impedance spectroscopy technique together with high-angle annular dark-field (HAADF)-STEM was used to investigate wake-up in HfO_2 films. The wake-up was attributed to phase transition from monoclinic to orthorhombic phase in bulk of the films as well as changes in or diminishment of tetragonal phase from electrode interfacial regions. In [34], the Raman spectroscopy technique was used to determine the phase composition of the layers. Such an irreversible phase conversion from nonpolar (monoclinic, cubic, or tetragonal phases) to polar (orthorhombic) phase manifests as an increase in the ferroelectric switching charge and thereby a similar increase in the saturation value of the polarization (P_s), which is also observed in [33] and [35]. Fig. 9(c) shows that the change in saturation polarization (P_s) is much lower compared to change in P_r. This suggests that the change in the total number of ferroelectric domains contributing to switching response is much smaller than the observed increase in P_r. Therefore, the contribution of these mechanisms to wake-up is likely to be lower in the early part of wake-up, which is characterized by shift and merging of current peaks rather than increase in the magnitude or width of the current peak. A similar observation can be made in Fig. 6 where the change in P_s as a function of doping is much smaller than the change in P_r.

The precise origin of domain pinning effect (shift in coercive field) is unclear. Such a shift in the coercive field has

Authorized licensed use limited to: IMEC. Downloaded on September 12,2022 at 07:24:23 UTC from IEEE Xplore. Restrictions apply.

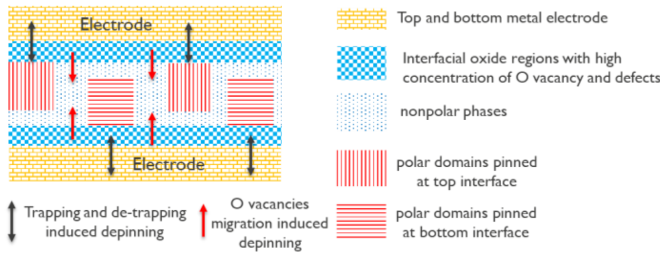

Fig. 10. Simplistic illustration of two groups of ferroelectric domains with pinning centers located at either top or bottom electrode interfaces. The wake-up process can be explained by either electron trapping and detrapping processes at the electrodes or redistribution of O vacancies.

been attributed to internal built-in electric field induced by the presence of charged defects and/or O vacancies [22], [24], [29]. In [22], three types of domains were observed in undoped HZO film using PFM measurements: 1) domains aligned to the applied electric field; 2) static (pinned or nonswitching) domains; and 3) anomalous domains with polarization aligned against the applied electric field. Here, the wake-up was attributed to the transformation of domains rather than phase transformation. The domain pinning and anomalous polarization reversal was attributed to the internal bias field created by oxygen vacancies. Electric field cycling was suggested to reduce the local density of oxygen vacancies, thereby reducing the internal bias field.

Looking at the dependence of the depinning process on direction of the electric field, the pinning centers are likely to be located near the top and bottom electrode interfaces. Fig. 10 shows a simplistic illustration of an MFM capacitor with two groups of domains with pinning centers located either at the top or bottom electrode interfaces. If pinning centers are charged, then the depinning process will involve discharging by trapping/detrapping electrons to and from the nearest metal electrode. The pinning effect can also be influenced by parameters that influence the number and distribution of O vacancies as well as defects. These parameters include electrodes, composition of the layer (stoichiometry of HZO, intentional dopants, as well as unintentional impurities), deposition, as well as annealing conditions. Subjecting the layers to fatigue cycles is suggested to result in redistribution of O vacancies, thereby gradual removal of built-in field that manifests as a shift in the coercive field.

The 3 Cy La doped HZO MFM capacitors were subjected to bipolar fatigue cycles with increase in the pulsewidth from 200 ns to 5 μs. Fig. 11 shows an impact of duration and amplitude of bipolar fatigue cycles on wake-up ($2P_r$) as a function of cycles and time. Fig. 11(b) shows that the initial P_r (up to 0.1 s) is independent of the frequency of the pulses, suggesting that this wake-up is mainly dominated by depinning of the domains. Above 0.1 s, $2P_r$ increases with increase in the duration of fatigue pulses suggesting the presence of additional wake-up mechanism such as phase conversion of nonferroelectric to ferroelectric phases [19], [20], [23].

Prolonged wake-up due to domain pinning effect can be addressed by precycling the devices at a higher electric field as shown in Fig. 12 where a capacitor was precycled at 3.2 MV/cm for 10^6 bipolar fatigue cycles. Later, this capacitor

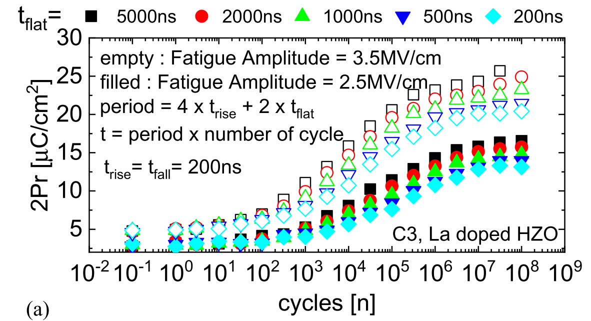

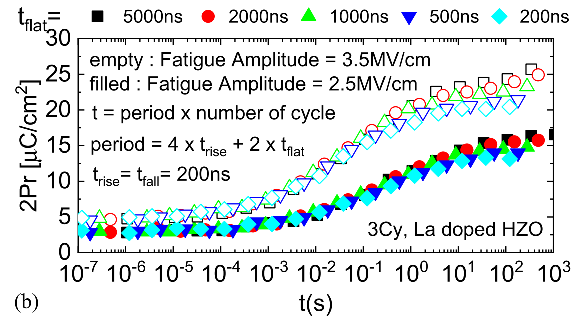

Fig. 11. Wake-up ($2P_r$) as a function of (a) number of cycles and (b) time for different durations of (200–5000 ns) and amplitude (2.5 and 3.5 MV/cm) of bipolar fatigue cycles. The initial wake-up (up to 0.1 s) is independent of frequency of the fatigue cycle.

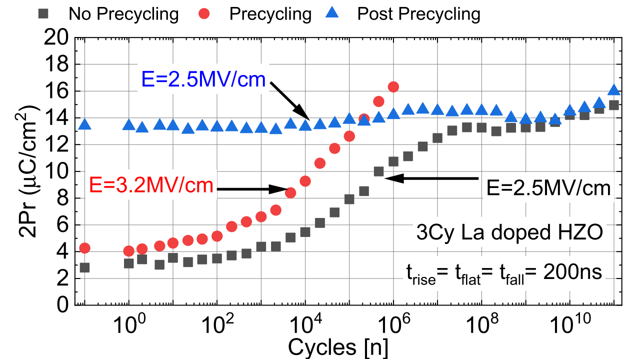

Fig. 12. Precycling (circles) at higher E (=3.2 MV/cm) offers earlier wake-up than lower E (=2.5 MV/cm) cycling (squares). Precycled sample shows relatively stable P_r until 10^{11} cycles upon further cycling (triangles) at a lower E of 2.5 MV/cm.

shows stable 2 P_r when operated at 2.5 MV/cm until 10^{11} cycles without any degradation in performance. Figs. 11 and 12 suggest that prolonged wake-up due to domain pinning can be potentially addressed by a global- or block-level precycling scheme at a cost of increased on-chip and/or off-chip circuitry. Moreover, such global one-time wake-up of an entire memory chip can be achieved within a time span of few seconds.

IV. Summary and Conclusion

High endurance (10^{11} cycles) La and Y doped ferroelectric HZO layers were demonstrated with Cl-based precursors. La doping is shown to offer higher remnant polarization than Y. Suppression of monoclinic phase was observed in doped layers that survive 10^{11} cycles. Investigation of doped layers with asymmetric polarization versus electric field (P–E) measurements and unipolar fatigue measurements suggests that in the pristine state, the HZO is comprised of two groups of ferroelectric domains with internal built-in electric field-induced

Authorized licensed use limited to: IMEC. Downloaded on September 12,2022 at 07:24:23 UTC from IEEE Xplore. Restrictions apply.

pinned coercive field (E_c). Doping is shown to increase the pinning effect and two distinct groups of ferroelectric domains emerge, which are antialigned at zero applied electric field (E). The antiferroelectric-like (pinched P–E loop) behavior is therefore attributed to internal built-in electric field-induced antialigned pinning of the domains during growth and/or annealing steps. The initial wake-up effect is attributed to gradual depinning of the domains with bipolar electric pulses. The initial wake-up is shown to be dependent on total duration and magnitude of bipolar electric pulses. Precycling at higher E field is demonstrated for early wake-up and subsequent stable operation at a lower field until 10^{11} cycles.

REFERENCES

[1] A. Kashir, S. Oh, and H. Hwang, "Defect engineering to achieve wake-up free HfO2-based ferroelectrics," *Adv. Eng. Mater.*, vol. 23, no. 1, Jan. 2021, Art. no. 2000791, doi: 10.1002/adem.202000791.

[2] S. Zarubin *et al.*, "Fully ALD-grown TiN/$Hf_{0.5}Zr_{0.5}O_2$/TiN stacks: Ferroelectric and structural properties," *Appl. Phys. Lett.*, vol. 109, no. 19, Nov. 2016, Art. no. 192903, doi: 10.1063/1.4966219.

[3] T. Mittmann, F. P. G. Fengler, C. Richter, M. H. Park, T. Mikolajick, and U. Schroeder, "Optimizing process conditions for improved $Hf_{1-x}Zr_xO_2$ ferroelectric capacitor performance," *Microelectron. Eng.*, vol. 178, pp. 48–51, Jun. 2017, doi: 10.1016/j.mee.2017.04.031.

[4] K. Tahara *et al.*, "Strategy toward HZO BEOL-FeRAM with low-voltage operation ($\leq$ 1.2 V), low process temperature, and high endurance by thickness scaling," in *Proc. Symp. VLSI Technol.*, Jun. 2021, pp. 1–2.

[5] M. H. Park *et al.*, "Study on the size effect in $Hf_{0.5}Zr_{0.5}O_2$ films thinner than 8 nm before and after wake-up field cycling," *Appl. Phys. Lett.*, vol. 107, no. 19, Nov. 2015, Art. no. 192907, doi: 10.1063/1.4935588.

[6] F. Mo *et al.*, "Low-voltage operating ferroelectric FET with ultra-thin IGZO channel for high-density memory application," *IEEE J. Electron Devices Soc.*, vol. 8, pp. 717–723, 2020, doi: 10.1109/JEDS.2020.3008789.

[7] S. De *et al.*, "Ultra-low power robust 3bit/cell $Hf_{0.5}Zr_{0.5}O_2$ ferroelectric FinFET with high endurance for advanced Computing-In-Memory technology," in *Proc. Symp. VLSI Technol.*, Jun. 2021, pp. 1–2.

[8] S. Zhang *et al.*, "Low voltage operating 2D MoS_2 ferroelectric memory transistor with $Hf_{1-x}Zr_xO_2$ gate structure," *Nanosc. Res. Lett.*, vol. 15, no. 1, p. 157, Aug. 2020, doi: 10.1186/s11671-020-03384-z.

[9] T. Francois *et al.*, "Demonstration of BEOL-compatible ferroelectric $Hf_{0.5}Zr_{0.5}O_2$ scaled FeRAM co-integrated with 130nm CMOS for embedded NVM applications," in *IEDM Tech. Dig.*, Dec. 2019, p. 15, doi: 10.1109/IEDM19573.2019.8993485.

[10] J. Okuno *et al.*, "High-endurance and low-voltage operation of 1T1C FeRAM arrays for nonvolatile memory application," in *Proc. IEEE Int. Memory Workshop (IMW)*, May 2021, pp. 1–3, doi: 10.1109/IMW51353.2021.9439595.

[11] P. D. Lomenzo, C.-C. Chung, C. Zhou, J. L. Jones, and T. Nishida, "Doped $Hf_{0.5}Zr_{0.5}O_2$ for high efficiency integrated supercapacitors," *Appl. Phys. Lett.*, vol. 110, no. 23, Jun. 2017, Art. no. 232904, doi: 10.1063/1.4985297.

[12] M. G. Kozodaev *et al.*, "Mitigating wakeup effect and improving endurance of ferroelectric HfO_2-ZrO_2 thin films by careful la-doping," *J. Appl. Phys.*, vol. 125, no. 3, Jan. 2019, Art. no. 034101.

[13] T. Song, R. Bachelet, G. Saint-Girons, R. Solanas, I. Fina, and F. Sánchez, "Epitaxial ferroelectric la-doped $Hf_{0.5}Zr_{0.5}O_2$ thin films," *ACS Appl. Electron. Mater.*, vol. 2, no. 10, pp. 3221–3232, Oct. 2020, doi: 10.1021/acsaelm.0c00560.

[14] M. Popovici *et al.*, "Ferroelectric La-Doped ZrO_2/$Hf_xZr_{1-x}O_2$ bilayer stacks with enhanced endurance," *Phys. Status Solidi (RRL) Rapid Res. Lett.*, vol. 15, no. 5, May 2021, Art. no. 2100033, doi: 10.1002/pssr.202100033.

[15] H. A. Hsain *et al.*, "Many routes to ferroelectric HfO_2: A review of current deposition methods," *J. Vac. Sci. Technol. A, Vac. Surf. Films*, vol. 40, no. 1, Jan. 2022, Art. no. 010803, doi: 10.1116/6.0001317.

[16] T. Schenk *et al.*, "About the deformation of ferroelectric hystereses," *Appl. Phys. Rev.*, vol. 1, no. 4, Dec. 2014, Art. no. 041103, doi: 10.1063/1.4902396.

[17] P. D. Lomenzo, M. Materano, C. Richter, R. Alcala, T. Mikolajick, and U. Schroeder, "A Gibbs energy view of double hysteresis in ZrO_2 and Si-doped HfO_2," *Appl. Phys. Lett.*, vol. 117, no. 14, Oct. 2020, Art. no. 142904, doi: 10.1063/5.0018199.

[18] S. Lombardo *et al.*, "Atomic-scale imaging of polarization switching in an (anti-)ferroelectric memory material: Zirconia (ZrO_2)," in *Proc. IEEE Symp. VLSI Technol.*, Jun. 2020, pp. 1–2, doi: 10.1109/VLSITechnology18217.2020.9265091.

[19] A. Chouprik *et al.*, "Ferroelectricity in $Hf_{0.5}Zr_{0.5}O_2$ thin films: A microscopic study of the polarization switching phenomenon and field-induced phase transformations," *ACS Appl. Mater. Interface*, vol. 10, no. 10, pp. 8818–8826, Mar. 2018, doi: 10.1021/acsami.7b17482.

[20] S. S. Fields *et al.*, "Phase-exchange-driven wake-up and fatigue in ferroelectric hafnium zirconium oxide films," *ACS Appl. Mater. Interface*, vol. 12, no. 23, pp. 26577–26585, Jun. 2020, doi: 10.1021/acsami.0c03570.

[21] Y.-J. Lin *et al.*, "Role of electrode-induced oxygen vacancies in regulating polarization wake-up in ferroelectric capacitors," *Appl. Surf. Sci.*, vol. 528, Oct. 2020, Art. no. 147014, doi: 10.1016/j.apsusc.2020.147014.

[22] A. Chouprik *et al.*, "Wake-up in a $Hf_{0.5}Zr_{0.5}O_2$ film: A cycle-by-cycle emergence of the remnant polarization via the domain depinning and the vanishing of the anomalous polarization switching," *ACS Appl. Electron. Mater.*, vol. 1, no. 3, pp. 275–287, Mar. 2019, doi: 10.1021/acsaelm.8b00046.

[23] S. Clima *et al.*, "First-principles perspective on poling mechanisms and ferroelectric/antiferroelectric behavior of $Hf_{1-x}Zr_xO_2$ for FEFET applications," in *IEDM Tech. Dig.*, San Francisco, CA, USA, Dec. 2018, pp. 16.5.1–16.5.4, doi: 10.1109/IEDM.2018.8614552.

[24] M. G. Kozodaev *et al.*, "Ferroelectric properties of lightly doped la:HfO_2 thin films grown by plasma-assisted atomic layer deposition," *Appl. Phys. Lett.*, vol. 111, no. 13, Sep. 2017, Art. no. 132903, doi: 10.1063/1.4999291.

[25] T. Schenk, M. Hoffmann, J. Ocker, M. Pešić, T. Mikolajick, and U. Schroeder, "Complex internal bias fields in ferroelectric hafnium oxide," *ACS Appl. Mater. Interface*, vol. 7, no. 36, pp. 20224–20233, Sep. 2015, doi: 10.1021/acsami.5b05773.

[26] P. D. Lomenzo *et al.*, "Harnessing phase transitions in antiferroelectric ZrO_2 using the size effect," *Adv. Electron. Mater.*, vol. 8, no. 1, Jan. 2022, Art. no. 2100556, doi: 10.1002/aelm.202100556.

[27] P. D. Lomenzo *et al.*, "AFE-like hysteresis loops from doped HfO_2: Field induced phase changes and depolarization fields," in *Proc. Joint Conf. IEEE Int. Freq. Control Symp. Int. Symp. Appl. Ferroelectr. (IFCS-ISAF)*, Jul. 2020, pp. 1–4, doi: 10.1109/IFCS-ISAF41089.2020.9234872.

[28] S. Clima *et al.*, "Ferroelectric switching in FEFET: Physics of the atomic mechanism and switching dynamics in $HfZrO_x$, HfO_2 with oxygen vacancies and Si dopants," in *IEDM Tech. Dig.*, Dec. 2020, pp. 4.2.1–4.2.4, doi: 10.1109/IEDM13553.2020.9372117.

[29] P. D. Lomenzo, C. Richter, T. Mikolajick, and U. Schroeder, "Depolarization as driving force in antiferroelectric Hafnia and ferroelectric wake-up," *ACS Appl. Electron. Mater.*, vol. 2, no. 6, pp. 1583–1595, Jun. 2020, doi: 10.1021/acsaelm.0c00184.

[30] F. Mehmood, T. Mikolajick, and U. Schroeder, "Lanthanum doping induced structural changes and their implications on ferroelectric properties of $Hf_{1-x}Zr_xO_2$ thin film," *Appl. Phys. Lett.*, vol. 117, no. 9, Aug. 2020, Art. no. 092902, doi: 10.1063/5.0021007.

[31] F. Mehmood, T. Mikolajick, and U. Schroeder, "Wake-up mechanisms in ferroelectric Lanthanum-Doped $Hf_{0.5}Zr_{0.5}O_2$ thin films," *Phys. Status Solidi (A)*, vol. 217, no. 22, Nov. 2020, Art. no. 2000281, doi: 10.1002/pssa.202000281.

[32] Y. Cheng *et al.*, "Reversible transition between the polar and antipolar phases and its implications for wake-up and fatigue in HfO_2-based ferroelectric thin film," *Nature Commun.*, vol. 13, no. 1, pp. 1–8, Feb. 2022, doi: 10.1038/s41467-022-28236-5.

[33] E. D. Grimley *et al.*, "Structural changes underlying field-cycling phenomena in ferroelectric HfO_2 thin films," *Adv. Electron. Mater.*, vol. 2, no. 9, Sep. 2016, Art. no. 1600173, doi: 10.1002/aelm.201600173.

[34] M. Materano *et al.*, "Raman spectroscopy as a key method to distinguish the ferroelectric orthorhombic phase in thin ZrO_2-based films," *Phys. Status Solidi (RRL) Rapid Res. Lett.*, vol. 16, no. 4, Apr. 2022, Art. no. 2100589, doi: 10.1002/pssr.202100589.

[35] T. Shimizu *et al.*, "Ferroelectricity mediated by ferroelastic domain switching in HfO_2-based epitaxial thin films," *Appl. Phys. Lett.*, vol. 113, no. 21, Nov. 2018, Art. no. 212901, doi: 10.1063/1.5055258.

Authorized licensed use limited to: IMEC. Downloaded on September 12,2022 at 07:24:23 UTC from IEEE Xplore. Restrictions apply.